Use of Finite Element Models for Determining Radiation Geometric View Factors

Patrick Edson
Victor Genberg

Eastman Kodak Company
Rochester, NY 14650-3118

ABSTRACT

Geometric view factor data is compared, using curved and planar surfaces, to determine the model detail necessary to accurately obtain radiation results for models of curved objects with planar finite elements. A finite cylinder with closed ends, for which the closed-form solution is known, is used as the reference. The results demonstrate that a moderately detailed mesh provides accurate solutions, allowing the use of a single condition and radiation model for models of this nature.

Introduction

Using finite elements as a complete solution in thermal analysis requires the accurate calculation of a radiation exchange matrix. Several tools are available which offer different techniques for determining geometrical view factors, and in turn, a radiation exchange matrix. The Radiant Energy Network Option (RENO) of the NEVADA Software Package [1] utilizes statistical ray tracing to calculate view factors. Benefits of this method include the ability to calculate the effect of highly reflective, specular surfaces, and the exact representation of curved surfaces (spheres, cylinders, cones, discs). A significant drawback in using this technique is the need to create a separate radiation model in addition to the finite element conduction model.

The methods available in MSC/NASTRAN [2] offer a contrasting set of advantages and disadvantages. The solutions available cannot incorporate the effect of specular finishes, and curved surfaces must be approximated by planar elements. However, only one model and analysis is required to solve the conduction and radiation portions of the problem. For large or complex models, this can potentially represent a significant savings in analysis and preprocessing time.

This paper addresses the issue of approximating curved surfaces with MSC/NASTRAN elements, such as CQUAD4 and CTRIA3 elements. With sufficient model detail, view factors determined with a finite element model should provide accurate solutions to thermal problems. To confirm this, results using MSC/NASTRAN are compared to a known exact solution to determine whether the level of model mesh fidelity necessary for accurate answers, and the resulting increase in preprocessing and solution time counters any gain in efficiency from using a single conduction and radiation model .

Sample Problem

Figure 1 shows a finite cylinder for which the closed form solution for the geometric view factors are readily available. Models are easily constructed for MSC/NASTRAN and RENO input, and the geometry contains two features of particular interest to this problem: a curved surface which *sees* itself, and a curved surface which sees a planar surface (and vice versa).

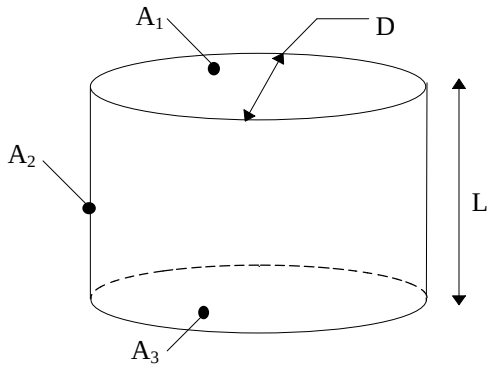

Figure 1 Finite Cylinder

The geometrical view factor F_{ij} between two any surfaces is determined by:

$$F_{ij} = \frac{1}{A_j} \int_{A_i} \int_{A_j} \frac{\cos\theta_i \cos\theta_j}{\pi R^2} dA_i dA_j , \qquad (1)$$

where A_i and A_j are arbitrarily oriented surfaces, which have a line of length R between the elemental areas dA_i and dA_j on each surface, and angles θ_i and θ_j between the surface normals and line R [3]. In addition, the summation rule states that:

$$\sum_{j=1}^{N} F_{ij} = 1 \tag{2}$$

A cylinder with L = 10 units and D = 20 units was used in the exact solution for comparison. The resulting view factors determined by Eq. (1) and Eq. (2) are listed in Table 1.

F_{13}	F_{31}	F_{12}	F_{32}	F_{21}	F_{23}	F_{22}
0.382	0.382	0.618	0.618	0.309	0.309	0.382

Table 1 Exact Solution Geometrical View Factors

Calculation Methods

Dividing surface 2 shown in Figure 1 into twelve elements circumferentially for an analysis model would create a suitable mesh for a conduction analysis of the cylinder. Therefore, the MSC/NASTRAN and RENO radiation models created have been created with the same fidelity. Five test cases were analyzed to determine the geometrical view factors:

(1) A RENO model using cylindrical section surfaces. Analyses with 2000, 4000, and 16000 rays were used.

(2) A RENO model using quadrilateral surfaces inscribed to the cylinder radius. Analyses with 2000, 4000, and 16000 rays were used.

(3) A RENO model using quadrilateral surfaces circumscribed to the cylinder radius. Analyses with 2000, 4000, and 16000 rays were used.

(4) An MSC/NASTRAN model using quad elements inscribed to the cylinder radius. Analyses were performed using CQUAD4 and CTRIA3 elements, and the VIEW module with 2x2, 6x6, and 10x10 subelement meshes. An analysis was also done using the VIEW3D module. A final analysis used CQUAD8 and CTRIA6 elements and the VIEW3D module.

(5) An MSC/NASTRAN model using CQUAD4 elements circumscribed to the cylinder radius. Analyses were performed using CQUAD4 and CTRIA3 elements, and the VIEW module with 2x2, 6x6, and 10x10 subelement meshes. An analysis was also done using the VIEW3D module. A final analysis used CQUAD8 and CTRIA6 elements and the VIEW3D module.

In case 1, the end caps were modeled as disc surfaces. In the remainder of the cases, triangle surfaces or elements were used for the end caps to complete the model. Figures 2 and 3 show the MSC/NASTRAN models viewed from the end cap, for the inscribed and circumscribed models respectively. RENO models using quadrilateral elements are constructed in the same manner.

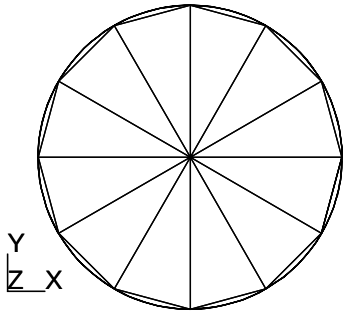

Figure 2 Inscribed Element and Surface Geometry

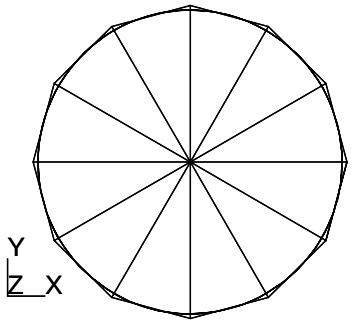

Figure 3 Circumscribed Element and Surface Geometry

Calculation Results

Tables 2 through 6 show the results of the five test cases. Each table includes the exact and model prediction values for the seven view factors listed in Table 1, as well as the relative error in the model prediction.

	Rays		2000		4000		16000
View	**Exact**	**Model**	**Error**	**Model**	**Error**	**Model**	**Error**
F13	0.3836	0.3625	-5.50%	0.3850	0.36%	0.3822	-0.36%
F31	0.3836	0.3805	-0.81%	0.3808	-0.73%	0.3801	-0.91%
F12	0.6180	0.6375	3.15%	0.6150	-0.49%	0.6178	-0.04%
F32	0.6180	0.6195	0.24%	0.6193	0.20%	0.6199	0.31%
F21	0.3090	0.3049	-1.33%	0.3061	-0.93%	0.3085	-0.18%
F23	0.3090	0.3115	0.79%	0.3098	0.26%	0.3104	0.44%
F22	0.3836	0.3836	0.43%	0.3840	0.52%	0.3811	-0.22%

Table 2 RENO Cylindrical Results (Case 1)

	Rays		2000		4000		16000
View	**Exact**	**Model**	**Error**	**Model**	**Error**	**Model**	**Error**
F13	0.3836	0.3791	-1.16%	0.3725	-2.90%	0.3736	-2.59%
F31	0.3836	0.3764	-1.86%	0.3737	-2.57%	0.3750	-2.24%
F12	0.6180	0.6209	0.46%	0.6276	1.54%	0.6263	1.34%
F32	0.6180	0.6236	0.90%	0.6263	1.34%	0.6250	1.13%
F21	0.3090	0.2988	-3.30%	0.3019	-2.30%	0.3043	-1.52%
F23	0.3090	0.3015	-2.42%	0.2999	-2.94%	0.2989	-3.26%
F22	0.3836	0.3995	4.17%	0.3981	3.79%	0.3967	3.43%

Table 3 Inscribed RENO Results (Case 2)

	Rays		2000		4000		16000
View	**Exact**	**Model**	**Error**	**Model**	**Error**	**Model**	**Error**
F13	0.3836	0.38825	1.22%	0.38429	0.19%	0.38275	-0.21%
F31	0.3836	0.38292	-0.17%	0.38119	-0.62%	0.38503	0.38%
F12	0.6180	0.61175	-1.02%	0.61572	-0.37%	0.61726	-0.12%
F32	0.6180	0.61708	-0.15%	0.61881	0.13%	0.61497	-0.50%
F21	0.3090	0.30421	-1.56%	0.31172	0.87%	0.30761	-0.46%
F23	0.3090	0.30792	-0.36%	0.30131	-2.49%	0.30627	-0.89%
F22	0.3836	0.38783	1.11%	0.38688	0.86%	0.38609	0.66%

Table 4 Circumscribed RENO Results (Case 3)

	Mesh		2x2		6x6		10x10
View	**Exact**	**Model**	**Error**	**Model**	**Error**	**Model**	**Error**
F13	0.3836	0.3804	-0.81%	0.3748	-2.29%	0.3743	-2.42%
F31	0.3836	0.3804	-0.81%	0.3748	-2.29%	0.3743	-2.42%
F12	0.6180	0.6120	-0.97%	0.6268	1.42%	0.6269	1.43%
F32	0.6180	0.6120	-0.97%	0.6268	1.42%	0.6269	1.43%
F21	0.3090	0.2956	-4.34%	0.3027	-2.04%	0.3028	-2.02%
F23	0.3090	0.2956	-4.34%	0.3027	-2.04%	0.3028	-2.02%
F22	0.3836	0.4041	5.34%	0.3966	3.40%	0.3959	3.21%

Table 5a Inscribed MSC/NASTRAN Results (Case 4)

	VIEW3D		QUAD4		QUAD8
View	**Exact**	**Model**	**Error**	**Model**	**Error**
F13	0.3836	0.3721	-3.00%	0.3815	-0.55%
F31	0.3836	0.3721	-3.00%	0.3815	-0.55%
F12	0.6180	0.6229	0.78%	0.6359	2.89%
F32	0.6180	0.6229	0.78%	0.6359	2.89%
F21	0.3090	0.3009	-2.61%	0.3072	-0.59%
F23	0.3090	0.3009	-2.61%	0.3074	-0.51%
F22	0.3836	0.3983	3.83%	0.3765	-1.85%

Table 5b Inscribed MSC/NASTRAN Results (Case 4)

	Mesh		2x2		6x6		10x10
View	**Exact**	**Model**	**Error**	**Model**	**Error**	**Model**	**Error**
F13	0.3836	0.3902	1.73%	0.3858	0.58%	0.3849	0.36%
F31	0.3836	0.3902	1.73%	0.3858	0.58%	0.3849	0.36%
F12	0.6180	0.6187	0.11%	0.6151	-0.47%	0.6153	-0.44%
F32	0.6180	0.6187	0.11%	0.6151	-0.47%	0.6153	-0.44%
F21	0.3090	0.3081	-0.30%	0.3063	-0.88%	0.3064	-0.86%
F23	0.3090	0.3081	-0.30%	0.3063	-0.88%	0.3064	-0.86%
F22	0.3836	0.3950	2.99%	0.3882	1.20%	0.3875	1.03%

Table 6a Circumscribed MSC/NASTRAN Results (Case 5)

	VIEW3D		QUAD4		QUAD8
View	**Exact**	**Model**	**Error**	**Model**	**Error**
F13	0.3836	0.3849	0.34%	0.3928	2.41%
F31	0.3836	0.3849	0.34%	0.3928	2.41%
F12	0.6180	0.6321	2.27%	0.6450	4.37%
F32	0.6180	0.6321	2.27%	0.6450	4.37%
F21	0.3090	0.3053	-1.19%	0.3116	0.84%
F23	0.3090	0.3053	-1.19%	0.3116	0.84%
F22	0.3836	0.3922	2.25%	0.3688	-3.86%

Table 6b Circumscribed MSC/NASTRAN Results (Case 5)

Conclusions

The results from Tables 5 and 6 demonstrate that accurate results from MSC/NASTRAN can be obtained without a highly detailed mesh that would add complexity to the model. In comparison to Table 1, which offers the most geometrically accurate representation of the cylinder, the error in prediction values is very close for the circumscribed model. Additionally, what is not displayed, and what could not be easily quantified, is the CPU time required by each method. However, in terms the amount of user time, the view factor calculations with MSC/NASTRAN were noticeably faster for the 10x10 subelement mesh, than even the 2000 ray RENO calculations.

Analyses of highly reflective surfaces still require that the analysis method allow elements to see secondary surfaces by reflection. When the extended capabilities of a package like RENO are necessary, as is the case with specular surfaces, the results from the case two models demonstrate that using quadrilateral and triangle surfaces in place of cylindrical and disk sections also provide results similar to MSC/NASTRAN in accuracy for both inscribed and circumscribed models.. Therefore, an intermediate solution is available, whereby a single model can be constructed using finite elements, and a RENO input file with surfaces based on the planar finite elements.

As an example of this intermediate solution for this paper, the RENO models which use quadrilateral surfaces were created directly from an MSC/PATRAN [4] model. First, the models used in the MSC/NASTRAN analysis were constructed in MSC/PATRAN. Second, an extension to MSC/PATRAN was then written using the PATRAN Command Language (PCL), that creates a RENO input deck from the MSC/PATRAN model. While this method still requires two analyses, it does eliminate the need for preprocessing two models.

It should be noted that these results are for one particular geometry. Further analyses are necessary to demonstrate that calculating view factors with finite elements will provide as accurate results for other non-planar shapes and models as well. In addition, variations such as a using different subelement meshes for different elements within the model would be useful in minimizing the number of subelements in geometries where they are not needed.

References

[1] *NEVADA User's Manual*, Turner Associates Consultants, Incline Village, NV, 1988

[2] *MSC/NASTRAN User's Manual*, Version 68, The MacNeal Schwendler Corporation, Los Angeles, CA, 1994

[3] Incropera, F. P., and De Witt, D. P.., *Introduction to Heat Transfer*, Second ed., John Wiley & Sons, Inc., 1990

[4] *MSC/PATRAN3 User's Manual*, Release 1.4-2. The MacNeal Schwendler Corporation, Los Angeles, CA, 1995

Appendix
Using MSC/NASTRAN for Integrated Thermal/Structural Analysis

Advantages

MSC/NASTRAN offers several advantages over traditional heat transfer techniques common in the aerospace industry. Many heat transfer analyses are still conducted using hand calculated conduction links and capacitance nodes which are then solved in an iterative solver such as SINDA. A few of the most important advantages of using MSC/NASTRAN over older techniques are provided below.

1) The analyst has full capability geometric pre-processors such as MSC/PATRAN to import CAD geometry, or create new geometry which are then meshed into a finite element model. This eliminates the expensive and error prone hand calculation and input of thermal networks.

2) Standard model checkout features are available such as free edges, duplicate grids, etc.

3) Conventional finite difference networks are usually limited to square patterns and do not create diagonal links which are important in obtaining accurate answers on real non-rectangular geometries.

4) Graphical output of temperature contours or element fluxes available in post-processors such as MSC/NASTRAN is required to understand and validate the model behavior.

5) A single model with limited modifications can be used for both thermal and structural analyses in many cases

New Capabilities

Version 68 of MSC/NASTRAN offers several new features and capabilities in the heat transfer solutions 153 and 159.

1) New thermal surface elements (CHBDYi) which may be used for radiation, forced convection, or free convection. A variety of new techniques are available for defining these elements.

2) Multicavity radiation allows a much more efficient calculation and input of the radiation view factor matrix.

3) Radiation may be defined as body-to-boundary condition (RADBC) which is more convenient than a radiation exchange matrix.

4) Time varying BC (TEMPBC) are more easily defined than in the old large conductor technique.

5) The new nonlinear solution algorithms are based on the nonlinear structural solutions so that the same NLPARM and TSTEPNL apply.

Desired Additions

As with any new capability there is more to be done to be fully effective. The following modifications would be very useful.

1) Add a thermostat element which operates like a household thermostat with a user specified dead band. (The current NOLIN capability has no deadband.) This is required for any thermal control problem. A nice feature for spacecraft thermal control, would include a user specified cycle time at which the control system is monitored.

2) The user needs more energy balance information to verify the models performance. Currently there is no output for energy flow to RADBC, lost to deep space, or the ambient point (ELEAMB) on RADCAV. An overall energy balance table would be very helpful.

3) Allow the user to specify modifications to the radiation matrix whether it is calculated inside MSC/NASTRAN or supplied on RADMTX entries. An automated feature to scale the matrix up or down to obtain a value of 1 which neither creates energy nor loses it to deep space.

4) Allow the user the option to input geometric view factors (f) on the RADMTX so that surface areas of CHBDY elements are not required by the user.

5) Throughout the documentation the difference between f, F and $\mathcal{F}$ should be clearly specified.

Thermal - Structural I/F

If the thermal model and the structural model have the same grid points and numbering scheme, then the interface for thermo-elastic analysis is seamless. In many cases and for many reasons, the thermal model and structural models do not have grid points in common. Usually the structural model has much more detail than the thermal model.

A common technique is to find the grid points in the structural model which are closest to the thermal points, constrain those points via SPCs to the thermal points' temperatures, and run the structural model as a thermal conduction model to find the other grid point temperatures. This technique is time consuming, error prone, and gives very poor quality answers in general.

A more automated and more accurate approach has been generated by Kodak. If the thermal model is represented as an MSC/NASTRAN model (only grid points and conduction elements are required) then the SINPST computer program uses finite element shape functions to interpolate temperatures to all of the intermediate structural grid points. This interpolation was described in Genberg, "Shape Function Interpolation of 2D and 3D Finite Element Results", MSC 1993 World Users Conference Proc. A capability such as this would be more useful and general if it were available in a geometric post-processor such as MSC/PATRAN.

Since MSC/NASTRAN does not have a thermostat element yet, our thermal control models are run in SINDA. Kodak has written a program (NASIN) to convert an MSC/NASTRAN model to a SINDA model. The conduction, capacitance and radiation matrices are output to a file which is then converted to SINDA conduction links, capacitance nodes, and radiation links. This approach takes advantage of finite element pre-processors to create the model, uses SINDAs solution capabilities, provides contour plot capability of results, and allows for automated interpolation of temperatures to a structural model. The issues involved are discussed in Handbook for Optics, Chapter 9, Thermal & Thermoelastic Analysis of Optics, by V. Genberg due for publication 8/96 by CRC Press.

It is hoped that MSC will offer a fully functional and automated thermal-structural analysis capability in the near future.